Electronic Supplementary Material (ESI) for Nanoscale.

Supporting Information for 'Ballistic heat transport in laser generated nano-bubbles'

June 22, 2016

1 Conservation equations for the van der Waals model

The natural order parameter for a liquid-vapor phase transition is the molecular density, and we shall focus below on the evolution of the density profile $\rho(r,t)$, where r is the radial variable and t is time. The density field, the velocity field $\boldsymbol{v}(r,t)$ and the temperature field $T(r,t)$ follow the three conservation equations (mass, momentum and energy conservation):

$$\frac{\partial \rho}{\partial t} + \boldsymbol{\nabla}.(\rho \boldsymbol{v}) = 0, \tag{1}$$

$$m\rho \left(\frac{\partial \boldsymbol{v}}{\partial t} + \boldsymbol{v}.\boldsymbol{\nabla}\boldsymbol{v} \right) = -\boldsymbol{\nabla}.\left(\boldsymbol{P} - \boldsymbol{D}\right), \tag{2}$$

$$m\rho c_v \left(\frac{\partial T}{\partial t} + \boldsymbol{v}.\boldsymbol{\nabla}T \right) = -l\boldsymbol{\nabla}.\boldsymbol{v} + \boldsymbol{\nabla}.(\lambda \boldsymbol{\nabla}T) + \boldsymbol{D} : \boldsymbol{\nabla}\boldsymbol{v} + \phi_{\mathrm{b}}\delta(\vec{r} - \vec{R}_b), \tag{3}$$

where m is the mass of a water molecule, c_v is the fluid specific heat, $l = T\left(\partial P/\partial T\right)_\rho$ is the Clapeyron coefficient (P is pressure) and λ the thermal conductivity. The two tensors $\boldsymbol{P}$ and $\boldsymbol{D}$ are the pressure tensor and the viscous stress tensor respectively. The last term in the energy equation eq. 3 is a ballistic heat flux when a bubble is present, and $\vec{R}_b$ denotes the location of the bubble surface.

To account for the liquid-vapor phase transition we use a density functional approach based on the van der Waals bulk free energy with an additional square gradient term to account for the finite thickness of the interface at the nanometer scale, and to include surface tension effects in the model [1, 2]. The resulting pressure tensor is a function of the local density in the fluid, $\rho(r,t)$ and its gradients:

$$P_{\alpha\beta} = \left[P_{\mathrm{VdW}} - w\rho\Delta\rho + \frac{w}{2}(\nabla\rho)^2 \right] \delta_{\alpha\beta} + w\partial_\alpha\rho\partial_\beta\rho. \tag{4}$$

Mass density kg/m^3	c_v kJ/(kg.K)	λ W/(m.K)	l Pa	$\eta = 3\mu/5$ Pa.s
997	4.13	0.606	5.4×10^{8}	8.98×10^{-4}
$2.22\ 10^{-2}$	1.44	0.019	6881	9.9×10^{-6}

Table 1: Parameter values used in the model. The top line corresponds to the liquid phase, the bottom to the vapor phase.

Here, P_{VdW} is the pressure obtained from the van der Waals theory:

$$P_{\mathrm{VdW}} = \frac{\rho k_B T}{1-\rho b} - a\rho^2.$$

The parameter w in (4) fixes the interface thickness and the surface tension. This parameter has been adjusted to match the surface tension of water at room temperature (T = 297 K). $\delta_{\alpha\beta}$ is the Kronecker symbol, and ∂_α is a derivative with respect to the spatial coordinate in the direction α. Δ is the Laplace operator. The two van der Waals parameters a and b have been chosen so that the density of the liquid phase at T = 297 K corresponds to the density of water, and the critical temperature is T_c = 647.3 K. With these ingredients, using a linear variation of c_v, l, λ, the shear and bulk viscosities η and μ across the liquid-vapor interface (written for η only below):

$$\eta(r) = \eta_{\mathrm{vap}} + \frac{\rho(r)-\rho_{\mathrm{vap}}}{\rho_{\mathrm{liq}}-\rho_{\mathrm{vap}}}(\eta_{\mathrm{liq}}-\eta_{\mathrm{vap}})$$

with the values in the liquid and vapor phases given in table 1.

Here, we show that the term $-l\vec{\nabla}\cdot\vec{v}$ is responsible for the liquid/vapor phase change. To do so, let us consider a volume of liquid and assume that we are working at constant temperature, and at the corresponding saturation pressure $P_{\mathrm{sat}}(T)$. Under these conditions, the change of enthalpy per mole of fluid corresponding to the liquid/vapor transition is :

$$\Delta H = \int_{t=0}^{t_{\mathrm{vap}}} \int_{\mathcal{V}} +l\vec{\nabla}\cdot\vec{v}d\vec{r}dt \qquad (5)$$

where we assumed that we started at time $t = 0$ the vaporization process, and t_{vap} is the time necessary to vaporize a mole of vapor. Using the mass conservation equation eq. 1, the enthalpy change may be rewritten :

$$\Delta H = \int_{t=0}^{t_{\mathrm{vap}}} \int_{\mathcal{V}} -\frac{l}{\rho}\frac{d\rho}{dt}d\vec{r}dt \qquad (6)$$

and if we further assume that the fluid properties are homogeneous on the local scale considered, $\mathcal{V} = N_a/\rho$, N_a being the Avogadro number, the change of enthalpy writes :

$$\Delta H = \int_{\rho_l}^{\rho_v} -\frac{l}{\rho^2}d\rho = N_a T\frac{dP_{\mathrm{sat}}}{dT}(v_{\mathrm{vap}}-v_{\mathrm{liq}}) = L \qquad (7)$$

which is exactly the Clausius-Clapeyron relation [3], with v_{liq} and v_{vap} the liquid and vapor specific volumes, and we have used the definition of the coefficient l : $l = T(\frac{dP_{\mathrm{sat}}}{dT})_\rho$.

The three equations (1), (2) and (3) are solved in the radial direction using a finite difference scheme for the spatial derivatives, and an Euler scheme for the time evolution. In addition, we implemented perfectly matched layers at the boundaries of the simulation cell, to avoid any spurious reflection of the acoustic wave generated by vaporization.

The choice of a continuum description for the fluid is dictated by the generation of a pressure wave due to the heat shock, that travels away from the nanoparticle in unbounded geometries, but may lead to spurious reflections and induce a premature bubble collapse in a finite geometry. To discard these boundary problems, we consider a quite large spherical system of radius 390 nm, centered on the nanoparticle of radius 10nm to 30 nm, and use at the boundaries of the system a Perfectly Matched Layers scheme to prevent any reflection of the pressure wave [4, 5]. Relying on the spherical geometry of the system, we restrict the study to spherosymmetrical solutions that allow a dimensional reduction of the problem to a 1D situation. This assumption is consistent with the metallic nature of the GNP where fast thermal transfer in the nanoparticle induces a homogeneous temperature field inside the particle, and with the spinodal nature of the vapor production that should occur at the same time at any location on the surface of the nanoparticle. We finally mention that the spherical geometry of the bubble is confirmed by molecular dynamics (MD) simulations [6], although it is not an assumption of MD.

2 Estimation of the dimensionless coefficient α

We discuss here the kinetic theory model to estimate the coefficient α, which appears in the expression of the ballistic flux ϕ_b in eq. 3. To estimate α, we use kinetic theory for a vapor phase between two boundaries, (the GNP surface at temperature T_{np} and the bubble surface in contact with the liquid phase at temperature T_G), see fig. 1. This simple model assumes that the vapor molecules are evaporated at the surface of the bubble, with a Boltzmann distribution of the velocities corresponding to the temperature T_G, hit the GNP surface and are reflected with a Boltzmann distribution corresponding to T_{np}.

For a slab geometry, as depicted in Fig. 1 a), a simple calculation leads to the expression of the average flux ϕ_{slab}:

$$\phi_{\mathrm{slab}} = \rho_{\mathrm{b}} \sqrt{\frac{(2k_B)^3}{\pi m}} \frac{\sqrt{T_{\mathrm{np}} T_G}}{\sqrt{T_{\mathrm{np}}} + \sqrt{T_G}} \left(T_{\mathrm{np}} - T_G\right),$$

with ρ_b the bulk density of the vapor phase. To arrive to this latter expression, it is assumed that all the molecules travelling from the GNP to the liquid vapor interface have been emitted with a temperature T_{np}, and all the particles travelling in the opposite direction have been evaporated with T_G. This is

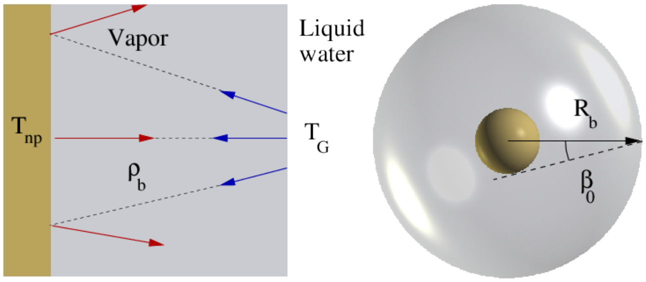

a) Slab geometry b) Spherical geometry

Figure 1: Sketch of the system used for the kinetic theory estimation of the accommodation coefficient. Figure a) is for a slab geometry while b) corresponds to the nanoparticle system.

not stricly speaking exact, because the two interfaces (GNP and Bubble) can produce specular reflections, where the particule is reflected with no change of kinetic energy. However, the probability of such an event is rather small [7]. Following the strategy presented in [8], it is possible to account for this effect by introducing an evaporation fraction α_{evap} that has been estimated in molecular simulations [9] to be on the order of $\alpha_{\mathrm{evap}} \simeq 0.35$.

Moreover, it is possible to take into account the spherical geometry relevant to nanobubbles by considering that only the molecules evaporated at the liquid vapor interface having a direction inside a cone with an angle β_0 (see Fig. 1 b)) can reach the GNP, so that the energy flux at the GNP surface is given by:

$$\phi = \frac{\alpha_{\mathrm{evap}}\rho_{\mathrm{b}}}{\sqrt{\pi m}} \frac{\sqrt{(2k_B)^3 T_{\mathrm{np}} T_G}\,(T_{\mathrm{np}} - T_G)}{(1+\cos\beta_0)\sqrt{T_{\mathrm{np}}} + (1-\cos\beta_0)\sqrt{T_G}}.$$

Comparison with eq. 3 in the main text leads to:

$$\alpha = \alpha_{\mathrm{evap}}\alpha_{\mathrm{geo}}\frac{\rho_{\mathrm{b}}}{\rho_{\mathrm{s}}},$$

with the following expression for α_{geo}:

$$\alpha_{\mathrm{geo}} \equiv \frac{2}{\sqrt{\pi}} \frac{\sqrt{T_{\mathrm{np}} T_G}\,(T_{\mathrm{np}} - T_G)\left(T_{\mathrm{np}}^{3/2} - T_G^{3/2}\right)^{-1}}{(1+\cos\beta_0)\sqrt{T_{\mathrm{np}}} + (1-\cos\beta_0)\sqrt{T_G}},$$

that depends on T_{np} and on the bubble size through the angle β_0 (T_G is room temperature). In practical conditions, the coefficient α_{geo} is found to vary slowly around $0.1 - 0.2$ (see Fig.2 and the text below). The GNP radius is chosen to match the experiments in [11] ($R_{\mathrm{np}} = 30$ nm) that we shall consider to compare with our results. Finally, the prefactor $\rho_{\mathrm{b}}/\rho_{\mathrm{s}}$ can be evaluated from the density profiles (see for instance Fig. 2 in the main text). For a contact angle $\theta = 50°$

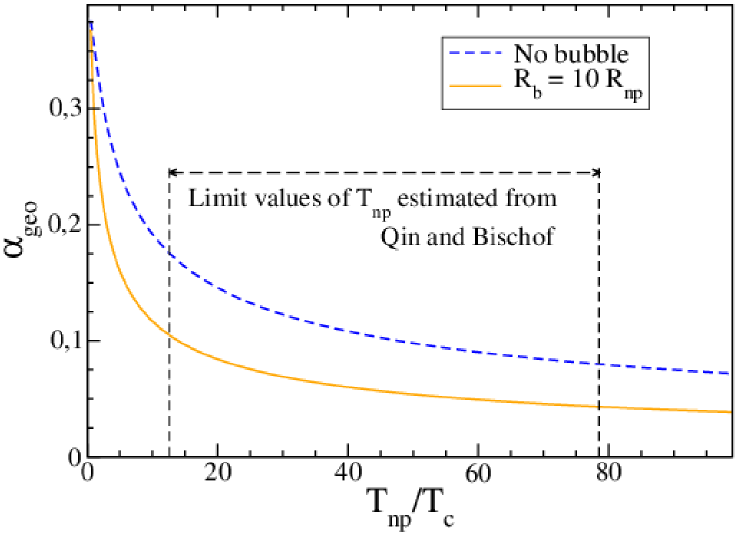

Figure 2: Variation of $\alpha_{\rm geo}$ with the GNP temperature for two extreme bubble sizes : $R_G = R_{\rm np}$(no bubble) and $R_G = 10\,R_{\rm np}$. The temperature range experimentaly used is indicated by the vertical dashed lines and have been obtained from [10].

we obtain a fraction $\rho_{\rm b}/\rho_{\rm s}$ on the order of 1/16. Hence, the range of values that we obtain for α covers the interval 2.2 10^{-3}- 4.4 10^{-3}.

In Fig. 2 we plot the variations of $\alpha_{\rm geo}$ with $T_{\rm np}$ by considering two limiting cases, $\beta_0 = \pi/2$ (vanishingly small bubble) and $\beta_0 = 0.1$ rad (bubble 10 times larger than the GNP). From Fig. 2 we conclude that the temperature of the particle gives values of $\alpha_{\rm geo}$ smaller than 1. We consider GNPs heated to very high temperatures [10], and the coefficient $\alpha_{\rm geo}$ is found to vary slowly around 0.1.

References

[1] D. M. Anderson, G. B. McFadden, and A. A. Wheeler, Annu. Rev. Fluid Mech. **30**, 139 (1998).

[2] J. S. Rowlinson and B. Widom, *Molecular Theory of Capillarity* (Oxford University Press, Oxford, 2002).

[3] R. Balian, *From microphysics to macrophysics* (Springer, Berlin, 2007).

[4] F. D. Hastings, J. B. Schneider, and S. L. Broschat, The Journal of the Acoustical Society of America **100**, 3061 (1996).

[5] F. Q. Hu, X. Li, and D. Lin, Journal of Computational Physics **227**, 4398 (2008).

[6] K. Sasikumar and P. Keblinski, The Journal of Chemical Physics **141**, 234508 (2014).

[7] M. Bond and H. Struchtrup, Phys. Rev. E **70**, 061605 (2004).

[8] J. Barrett and C. Clement, Journal of Colloid and Interface Science **150**, 352 (1992).

[9] M. Matsumoto, Fluid Phase Equilibria **125**, 195 (1996), asian Thermophysical Properties Conference.

[10] Z. Qin and J. C. Bischof, Chem. Soc. Rev. **41**, 1191 (2012).

[11] A. Siems, S. A. L. Weber, J. Boneberg, and A. Plech, New Journal of Physics **13**, 043018 (2011).